

New Single-Switch Three-Phase High-Power-Factor Rectifiers Using Multiresonant Zero-Current Switching

Yungtaek Jang, *Member, IEEE*, and Robert W. Erickson, *Member, IEEE*

Abstract— A new family of single-switch three-phase high-power-factor rectifiers, which have continuous input and output currents, is introduced. By using a multiresonant scheme, the transistor operates with zero-current switching (ZCS), and the diodes operate with zero-voltage switching (ZVS). These multiresonant rectifiers with a single transistor are capable of drawing a higher quality input-current waveform at nearly unity power factor and lower stresses than quasi-resonant rectifiers. Buck-type converters are used for the power stage, and, hence, the output voltage is lower than the input voltage. Moreover, these rectifiers have a wide load range and low stresses on semiconductor devices. From the analysis, normalized characteristics of the rectifier are derived. The design and breadboard implementation of the rectifier delivering 147 V_{dc} at 6 kW from a 3 ϕ 240-V_{rms(LL)} input is described. The total harmonic distortion (THD) of the line current is less than 5%, and the system efficiency is about 94% at the full load.

Index Terms— Frequency control, multiresonant, power factor correction (PFC), resonant converters, three-phase rectifiers, zero-current switching.

I. INTRODUCTION

NUMEROUS publications [1]–[9] have treated the power-factor correction of three-phase ac-to-dc power supplies. Three-phase high-power-factor (HPF) pulse-width-modulated (PWM) rectifiers based on the discontinuous-conduction-mode (DCM) operation have been introduced and analyzed in [1]–[4]. However, HPF PWM boost-type rectifiers have a higher output voltage than the peak input voltage together with a pulsating output current. Moreover, the switching power loss puts a practical upper bound on the usable frequency range.

The quasi-resonant zero-current-switching (ZCS) HPF buck-type rectifiers have been introduced in [2] and [5]. It was shown in [2] that even though a resonant circuit is used, the transistor currents are lower than those in an equivalent three-phase HPF PWM rectifier. In addition, the ZCS property makes this approach well suited for applications employing insulated gate bipolar transistors (IGBT's). However, the buck-type rectifiers in [2] have pulsating input currents and, hence, require an extra input filter. The quasi-resonant zero-voltage-switching (ZVS) boost-type rectifiers of [6] exhibit

Manuscript received March 18, 1996; revised March 14, 1997. Recommended by Associate Editor, P. Enjeti.

Y. Jang is with Delta Power Electronics Laboratory, Inc., Blacksburg, VA 24060 USA.

R. W. Erickson is with the Department of Electrical and Computer Engineering, University of Colorado, Boulder, CO 80309-0425 USA (e-mail: rwe@boulder.colorado.edu).

Publisher Item Identifier S 0885-8993(98)00486-4.

nonpulsating input currents, but load-current variations lead to high transistor-voltage stress.

In this paper, a new family of three-phase single-switch HPF multiresonant buck-type rectifiers, which have continuous input and output currents, is introduced. Fig. 1 shows the three-phase multiresonant ZCS cell and the voltage waveshape of input-side resonant capacitor C_r . By using a multiresonant scheme, the transistor operates with ZCS, and the diodes operate with ZVS. Moreover, these multiresonant rectifiers with a single transistor are capable of drawing a higher quality input-current waveform at nearly unity power factor and lower stresses than the quasi-resonant rectifiers or the DCM PWM boost-type rectifiers. This is true because the portions of periods B and C in a switching interval as shown in Fig. 1(c) are shorter than those of the other types of topologies. Hence, the dominance of period A , when voltage V_{Cr1} is proportional to the input current, produces a more linear input characteristic. Buck-type converters are used for the power stage, and, hence, the output voltage is lower than the input voltage. These rectifiers have a wide load range and low stresses on the semiconductor devices. The design and breadboard implementation of this rectifier delivering 147 V_{dc} at 6 kW from a 3 ϕ 240-V_{rms(LL)} input is described. Experimental results demonstrate total harmonic distortion (THD) of less than 5% at the full load, less than 3.5% at 50% load, and less than 2% at 10% load in an open-loop rectifier. The rectifier efficiency is about 94% at the full load.

In Section II, benefits and special characteristics of the three-phase single-switch HPF multiresonant buck-type rectifiers are briefly discussed and compared with those of the HPF rectifiers based on quasi-resonant rectifiers and DCM PWM boost-type rectifiers. The principal operation of the proposed rectifier is presented in Section III.

In Section IV, the rectifier is analyzed, and the analysis results are presented as graphical forms. Special properties of the multiresonant topology for the high power factor are also explained.

In Section V, a design procedure for the rectifier is described. Extensive experimental results at 6 kW are reported in Section VI that verify the rectifier performance.

II. BENEFITS AND SPECIAL CHARACTERISTICS

Fig. 1 shows the three-phase multiresonant ZCS cell and the voltage waveshape of input-side resonant capacitor C_r . Filter

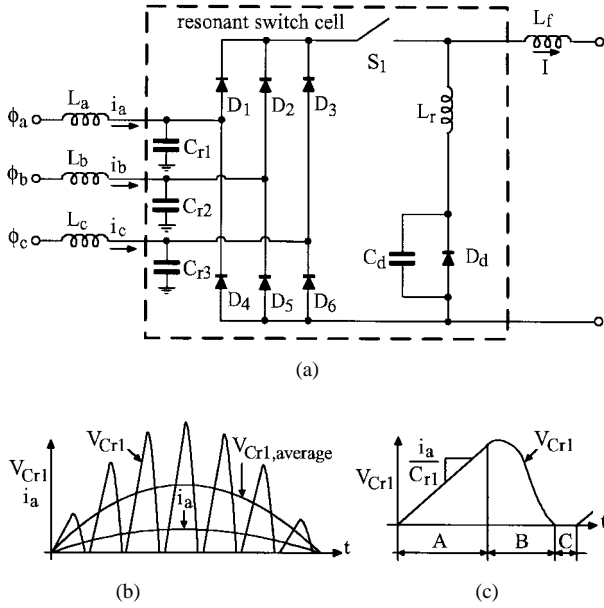


Fig. 1. (a) New three-phase multiresonant ZCS cell. (b) The input-side resonant-tank capacitor-voltage waveform together with the input-current waveform. (c) The enlarged waveform of V_{Cr1} during one switching period.

inductors $L_a, L_b, L_c,$ and L_f have small switching-frequency current ripples. In a steady state, the average voltage of C_r during a switching period is the same as the input voltage. Moreover, the peak voltage of C_r is proportional to the input current. If switching frequency f_s is much higher than input line frequency f_L , then the input-current waveshape will follow the input-voltage waveshape. Hence, this phenomenon results in a high power factor and a low harmonic input-current characteristic.

From Fig. 1(c), the resonant-voltage waveshape of V_{Cr1} is divided into three different periods. During the first period, V_{Cr1} is increasing linearly with the slope proportional to input current i_a . During the second period, resonant capacitor C_r is ringing together with resonant inductor L_r until V_{Cr1} reaches zero voltage. Finally, V_{Cr1} remains at zero for the third period. Hence, if the first period is longer than the sum of the second and the third periods, then the input-current waveshape becomes more proportional to the input-voltage waveform. Indeed, it is a good design if the first period is longer than the second and third periods. Therefore, these multiresonant rectifiers are capable of drawing a high-quality input-current waveform at nearly unity power factor with a single transistor.

Fig. 2 shows the basic circuit diagram and ideal waveforms of the single-switch three-phase multiresonant buck-type rectifier. Inductance L_r and capacitors $C_{r1}-C_{r3}$ and C_d form the multiresonant tank circuit and lead to ZCS in the transistor and ZVS in the diodes. Moreover, the voltage waveforms of resonant capacitors $C_{r1}-C_{r3}$ are pulsating sinusoidal with peaks proportional to the input line currents. This property yields an average or a low-frequency component in the line current approximately proportional to the phase voltage. Hence, the low harmonic rectification is obtained.

The converter is basically a buck topology, with an output voltage controllable between zero and approximately the peak

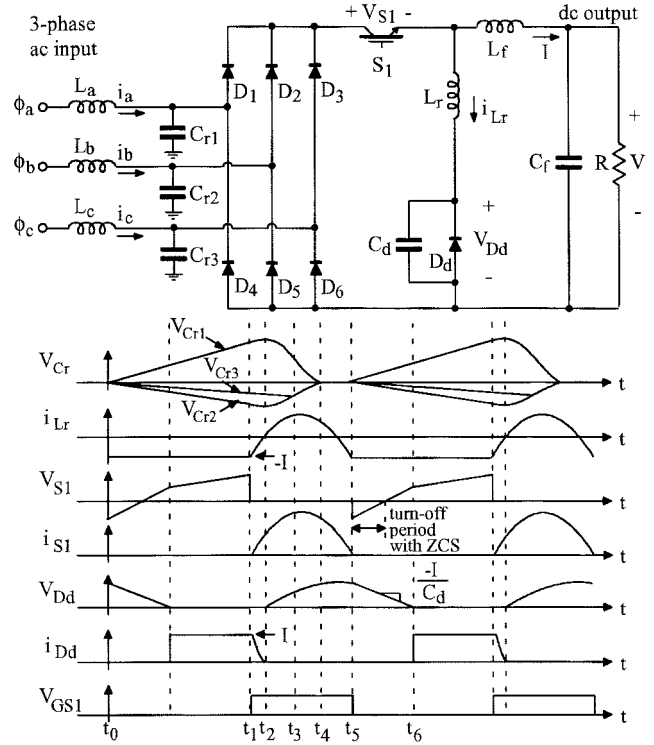


Fig. 2. The basic converter circuit and ideal waveforms of the new single-transistor three-phase multiresonant ZCS HPF rectifier.

ac line-to-line input voltage. Similar converters based on other dc-to-dc parent converters, which have different voltage-conversion ratios, were derived in [7].

The proposed rectifiers have a number of advantageous properties.

- 1) High-power-factor low-harmonic rectification is performed naturally.
- 2) Input and output currents are continuous.
- 3) Because of the buck-type rectifier property, the output voltage is lower than the peak line-to-line input voltage.
- 4) Wide range of the load power variation is achieved without excessive stresses.
- 5) A single switch operating at ZCS with good switch utilization is required.
- 6) Since the switch-on time is almost constant for the entire output load range, the control of the switch-off time is only required for the variable-frequency control of the rectifier.

III. PRINCIPLE OF OPERATION

To analyze the three-phase single-switch multiresonant ZCS buck rectifier shown in Fig. 2, it is sufficient to consider a 30° interval of the ac input line waveform, assuming the three-phase input voltages are symmetric and well balanced, and the switching frequency is much higher than the input line frequency. The 30° interval, where $i_a > 0 > i_c > i_b$, is described here.

1) Interval 1: $t_0 \leq t \leq t_1$, All Switches Are OFF Except D_d : In this interval, each tank capacitor $C_{r1}-C_{r3}$ charges up linearly at a rate proportional to its respective line current.

This will continue until switch S_1 is turned on. During this interval, resonant-tank inductor L_r supplies the output load current. When switch S_1 turns on, the bridge rectifier input line-to-line voltage V_{ab} is maximum, forcing D_1 and D_5 to conduct.

2) *Interval 2: $t_1 \leq t \leq t_2$, D_1 , D_5 , D_d , and S_1 Are ON:* In this interval, capacitor voltage V_{Cr3} continues to increase, while the other two capacitor voltages ring with resonant-tank inductor L_r until the tank inductor current increases to zero from the negative output current. Then, diode D_d turns off, initiating the next interval.

3) *Interval 3: $t_2 \leq t \leq t_3$, D_1 , D_5 , and S_1 Are ON:* In this interval, capacitor voltage V_{Cr3} continues to increase, while the other two capacitor voltages ring with resonant-tank inductor L_r . This will continue until V_{Cr3} becomes equal to V_{Cr2} . Diode D_6 then also conducts.

Depending on the magnitudes of i_b and i_c , the order of interval 2 and 3 may be reversed. Interval 3 occurs before interval 2 when currents i_b and i_c are similar in magnitude.

4) *Interval 4: $t_3 \leq t \leq t_4$, D_1 , D_5 , D_6 , and S_1 Are ON:* In this interval, resonant-tank capacitors $C_{r1}-C_{r3}$, parallel capacitor C_d , and resonant-tank inductor L_r form a resonant-tank circuit. This interval ends when the resonant-tank capacitor voltages $V_{Cr1}-V_{Cr3}$ discharge to zero.

5) *Interval 5: $t_4 \leq t \leq t_5$, All Switches Are ON Except D_d :* In this interval, parallel capacitor C_d and resonant-tank inductor L_r ring until the tank inductor current decreases to the negative load current. At this point, the input bridge rectifiers become reverse biased. Hence, the switch current becomes zero.

6) *Interval 6: $t_5 \leq t \leq t_6$, All Switches Are OFF:* Interval 6 is actually a subset of Interval 1 as shown in the waveforms of Fig. 2. The voltage of capacitor C_d linearly decreases until it reaches zero voltage and diode D_d turns on.

During the input bridge rectifiers are reverse biased, the complete load current is supplied by parallel capacitor C_d , therefore, switch S_1 can be turned off with ZCS as shown in Fig. 2.

IV. ANALYSIS

A. Approximate Simplified Model

According to the symmetry of the three-phase input voltages, the system behavior of the entire line period can be described by the extension of the interval $[0, \pi/6]$. To simplify the three-phase input and single-ended output circuit shown in Fig. 2, one operating point at the time $\pi/2$ is chosen. At this moment, phase voltage V_{an} is at its peak value. Phase voltages V_{bn} and V_{cn} are both negative and equal in magnitude to one half of V_{an} . Hence, capacitors C_{r2} and C_{r3} (shown in Fig. 2) are charged and discharged exactly in the same manner at this condition, and capacitors C_{r2} and C_{r3} can be considered as parallel-connected capacitors. Also, phase current i_{an} is at its peak value, while i_{bn} and i_{cn} are both one half of the negative phase current i_{an} . Therefore, the input-voltage sources and the input-filter inductors can be replaced by current source I_g as shown in Fig. 3, where I_g is the peak-phase current $i_{an-peak}$. Input-side resonant capacitors $C_{r1}-C_{r3}$ can be replaced by an

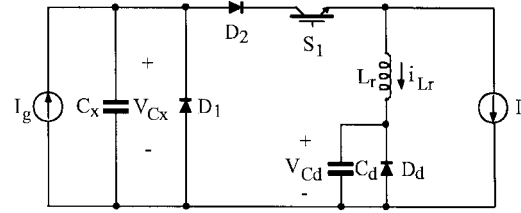


Fig. 3. The simplified single-input and single-output model of the new single-transistor three-phase multiresonant ZCS HPF rectifier.

effective capacitor C_x , which is equal to the series connection of C_{r1} and parallel-connected C_{r2} and C_{r3} . Diodes D_1 and D_2 of Fig. 3 represent the three-phase input bridge diodes. The output filter inductor is replaced by current source I . Finally, the simplified single-input and single-ended circuit diagram is shown in Fig. 3.

The relations between the actual three-phase input circuit and this simplified single-input and single-ended output model are given approximately as follows: 1) $C_x = C_r \times 2/3$, where input-resonant capacitors $C_{r1}-C_{r3}$ have the same values and are represented as C_r ; 2) $I_g =$ peak phase current $i_{an-peak}$; 3) $V_g = 3/2$ times peak-phase voltage $V_{an-peak}$, where V_g is also the same as the average voltage of V_{Cx} during one switching period; and 4) three-phase input power $P_{in} = V_g \times I_g = 3/2 \times V_{an-peak} \times i_{an-peak}$.

B. Normalization Based on Simplified Model

In this section, the converter equations are normalized with respect to the dc output voltage instead of the ac input voltage. This allows the system waveforms to be expressed as functions of the dc operating point. The normalizing base quantities are then described as V , I_0 , R_0 , and f_0 . The values for the normalizing quantities can be determined by the following:

$$\begin{aligned} \text{base voltage} &= V; \\ \text{base current } I_0 &= V/R_0; \\ \text{base impedance } R_0 &= \sqrt{\frac{L_r}{C_x}}; \\ \text{base frequency } f_0 &= \frac{1}{2\pi\sqrt{L_r C_x}} \end{aligned}$$

where V is the output voltage of the rectifier. Hence, if the rectifier is an ideal loss-free system, then the normalized values of the input and output quantities are described as $M_g = V_g/V$, $J_g = I_g R_0/V$, $J = I R_0/V = M_g J_g$, $\alpha = 2\pi f_0(t_1 - t_0)$, $\beta = 2\pi f_0(t_5 - t_1)$, and $\gamma = (\alpha + \beta)/2$, where $t_1 - t_0$ is the off time of switch S_1 and $t_5 - t_1$ is the on time of switch S_1 as shown in Fig. 2. Detailed derivations can be found in [8].

C. Analysis Results

Analysis results are shown in Figs. 4 and 5 in graphical forms. Fig. 4 shows the normalized input characteristic of the converter, i.e., normalized peak input current J_g versus normalized peak input voltage M_g for a given α . The normalized switch-off time α is the control variable for this rectifier. The switch-on period is essentially constant for the complete output

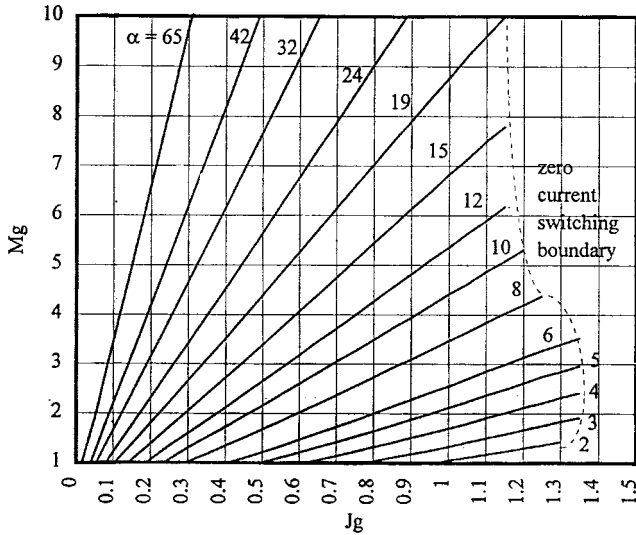


Fig. 4. The normalized input characteristic of the new single-transistor three-phase multiresonant ZCS HPF rectifier. The normalized transistor off time α is expressed in radians.

load range. Therefore, one can set the switch-on period as a constant value and control the switch-off period α .

The characteristics of Figs. 4 and 5 end for large J_g at the ZCS boundary. The ZCS property is lost at large normalized currents. Also, the characteristics are not plotted for M_g less than the unity because the multiresonant buck rectifier does not function when $M_g < 1$, i.e., when $V_g = 3/2 \times V_{an-peak}$ is less than the dc output voltage V .

Fig. 4 is useful for determining the converter steady-state operating point. Given a specified range of values of peak input voltage and load current, the range of variations of M_g and J_g can be determined from the definitions of Section IV-A and Section IV-B, and this region is overlaid on Fig. 4. The range of variation of the control parameter α can then be read graphically from the figure. The range of variations of switching period $\gamma = (\alpha + \beta)/2$ can then be estimated since switch conduction angle β is nearly constant and is typically approximately one half of the tank resonant period or π radians. Therefore, the switching frequency is approximately $f_s \approx 2\pi f_0 / (\alpha + \pi)$, and the normalized switching frequency F is $f_s / f_0 \approx 2\pi / (\alpha + \pi)$.

Fig. 5 shows the normalized voltage stress and the normalized current stress of switch S_1 and output diode D_d at different operating conditions. Again, the voltages and the currents are normalized using the base quantities defined in Section IV-B. The voltage stress of switch S_1 is shown in Fig. 5(a), and the current stress of switch S_1 is shown in Fig. 5(c). The voltage stress of switch S_1 is near constant for the entire load range. Moreover, at large voltage conversion ratios, the current stress of switch S_1 decreases at light loads. Fig. 5(b) shows the voltage stress of the output diode. The current stress of the resonant-tank inductor can also be found by subtracting normalized output current J ($M_g \times J_g = J$) from this current stress of the switch. The output diode voltage stress is the same as the voltage stress of C_d as shown in Fig. 5(b), and the current stress of the output diode is approximately equal to the output current.

V. DESIGN

A. Specification

- Input voltage 3ϕ ac 240 V (L-L, rms);
- Output voltage dc 147 V;
- Output power 6 kW–600 W.

From the specification, effective input voltage

$$V_g = \frac{3}{2} \times V_{an-peak} = \frac{3}{2} \times \frac{240\sqrt{2}}{\sqrt{3}} = 294 \text{ V}$$

and, hence, normalized input voltage

$$M_g = \frac{V_g}{V} = \frac{294}{147} = 2.$$

From Fig. 4, normalized input current J_g can be chosen to be as large as 1.36 for the maximum output power 6 kW and 0.136 for the 10% output power 600 W. Normalized frequency F is $2\pi / (\alpha + \pi) \approx 0.99$ at the maximum output power and 0.21 at the 10% load. Output current I becomes $P_{out} / V = 40.8$ A for the 6-kW output power, and, hence, the characteristic impedance is

$$R_0 = M_g J_g \frac{V}{I} = 2 \times 1.36 \times \frac{147}{40.8} = 9.8 \Omega$$

where R_0 is $\frac{JV}{I}$ and J is $M_g J_g$. If the maximum switching frequency for the 6-kW output power is chosen to be 90 kHz, then the resonant frequency f_0 can be calculated as

$$f_0 = \frac{f_s}{F} = \frac{90}{0.99} = 91 \text{ kHz}$$

where normalized frequency F is switching frequency f_s divided by resonant frequency f_0 . Hence, the minimum switching frequency at 10% load becomes $f_s = f_0 \times F = 91 \times 0.21 = 19.1$ kHz. From the above results, characteristic impedance

$$R_0 = \sqrt{L_r / C_x} = 9.8 \Omega$$

and base frequency

$$f_0 = \frac{1}{2\pi\sqrt{L_r C_x}} = 91 \text{ kHz},$$

Effective capacitance C_x is calculated to be 178 nF, and resonant-tank inductor L_r becomes 17 μ H. Therefore, input-side resonant-tank capacitors C_{r1} – C_{r3} are 268 nF, and the value of the output-side resonant-tank capacitor C_d is chosen to be equal to $C_x = 2/3 \times C_r$ or 178 nF. This choice leads to a good compromise between low transistor-voltage stress and low input-current harmonics.

From Fig. 5(a), the peak value of the normalized voltage stress of switch S_1 is shown to be 4.8 at M_g of 2 and J_g of 0.7. Hence, the peak switch voltage can be calculated as $V_{S1} = M_{S1} \times V = 4.8 \times 147 \text{ V} = 706 \text{ V}$ over the output load range. From Fig. 5(c), the peak value of the normalized current stress of switch S_1 is shown to be 5.2 at M_g of 2 and J_g of 1.36. Hence, the peak switch current can be calculated

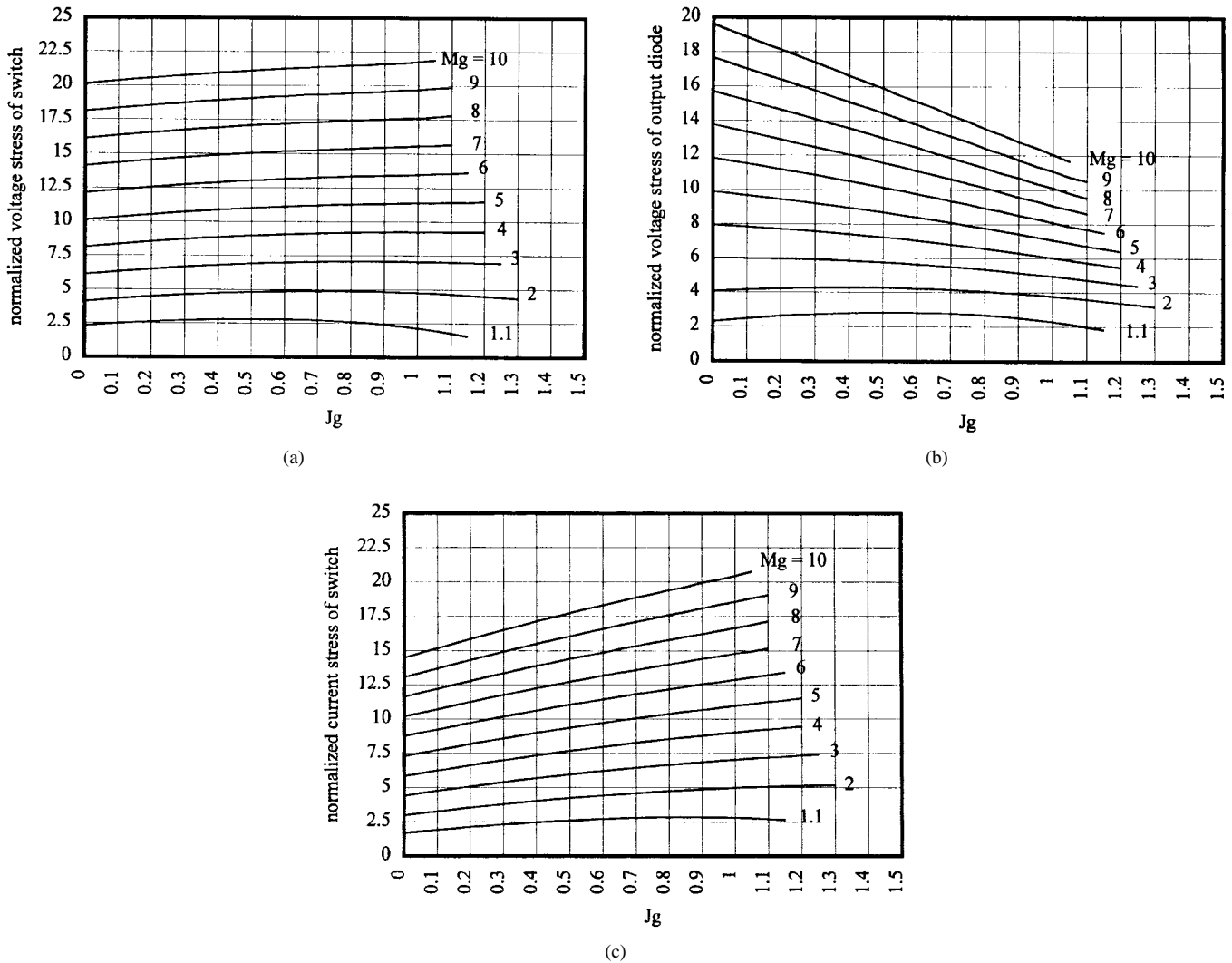


Fig. 5. The normalized stresses of the new single-transistor three-phase multiresonant ZCS HPF rectifier: (a) voltage stress of switch S_1 , (b) voltage stress of output diode D_d , and (c) current stress of switch S_1 . The current stress of the output diode is equal to the output current.

as $I_{S1} = J_{S1} \times V / R_0 = 5.2 \times 147 / 9.8 = 78$ A over the output load range. From Fig. 5(b), the peak value of the normalized voltage stress of output diode D_d is shown to be 4.2 at M_g of 2 and J_g of 0.4. Hence, the peak output diode voltage can be calculated as $V_{Dd} = M_{Dd} \times V = 4.2 \times 147 = 617$ V over the output load range. The current stress of the output diode is equal to the output current.

VI. EXPERIMENTAL RESULTS

The single-switch three-phase multiresonant ZCS HPF buck-type rectifier as shown in Fig. 2 was built. The output voltage V is 147 V_{dc} from a three-phase input voltage of 240 V_{rms(L-L)}. The maximum output power 6 kW is obtained at the switching frequency 89.3 kHz with switch-conduction time 6.5 μ s; the 50% output power of 3 kW is obtained at the switching frequency of 68 kHz with switch-conduction time 6.5 μ s; and the 10% output power 600 W is obtained at the switching frequency of 19.2 kHz with switch-conduction time 6.5 μ s. Input filter inductors $L_a, L_b,$ and L_c are 0.5 mH each, and output filter inductor L_f is 2 mH. Input-side resonant-

tank capacitors $C_{r1}-C_{r3}$ are connected in a Y configuration with 270 nF each. The value of the output-side resonant-tank capacitor C_d is chosen to be equal to $C_x = 2/3 \times C_r$ or 180 nF. Resonant-tank inductor L_r is 17 μ H. Hence, resonant frequency f_0 is 91 kHz, and characteristic impedance R_0 is 9.72 Ω . The load resistance $R_L = 3.6 \Omega$ is connected for the maximum load, $R_L = 7.2 \Omega$ is connected for the 50% load, and $R_L = 36 \Omega$ is connected for the 10% load.

Figs. (6)–(8) show the measured waveforms of input line current i_a with its ac phase voltage V_{an} together with the spectral analysis of the measured input current at three different load conditions.

Table I shows the measured stresses of the switch and the output diode at three different load conditions. Table II shows the measured rms harmonic currents of the line input current. A spectrum analyzer was used to measure the magnitudes of the harmonics, which are contained in the input line current. The THD of the input current is calculated numerically based on this measurement. The percentage of the THD was calculated for the first ten significant harmonics (2nd–11th).

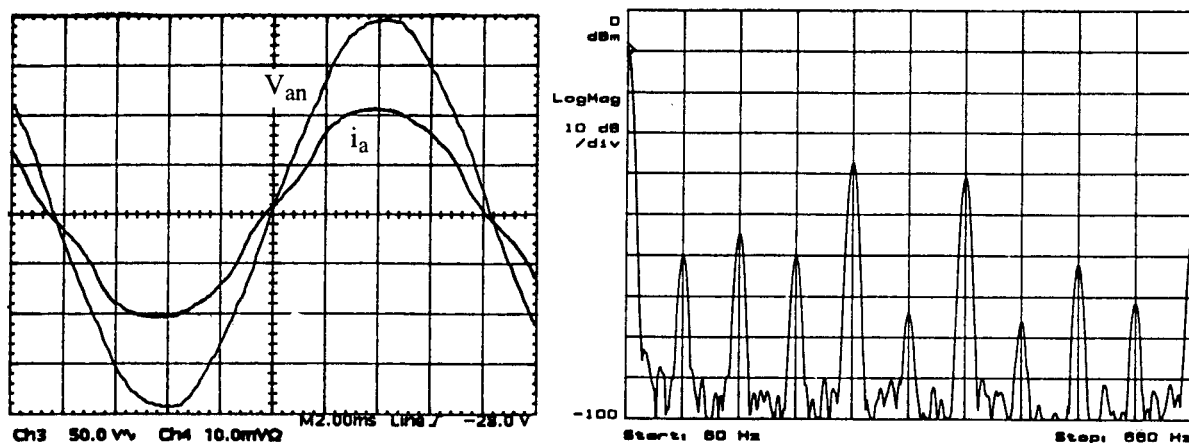


Fig. 6. Measured waveforms (vertical scale: 50 V/div, 10 A/div, and horizontal scale: 2 ms/div) and spectral analysis (vertical scale: 10 dB/div and horizontal scale: 60 Hz/div) of input line current i_a with its ac phase voltage V_{an} for the rectifier at 6-kW output power. The fundamental component of the input current is 14.9 A.

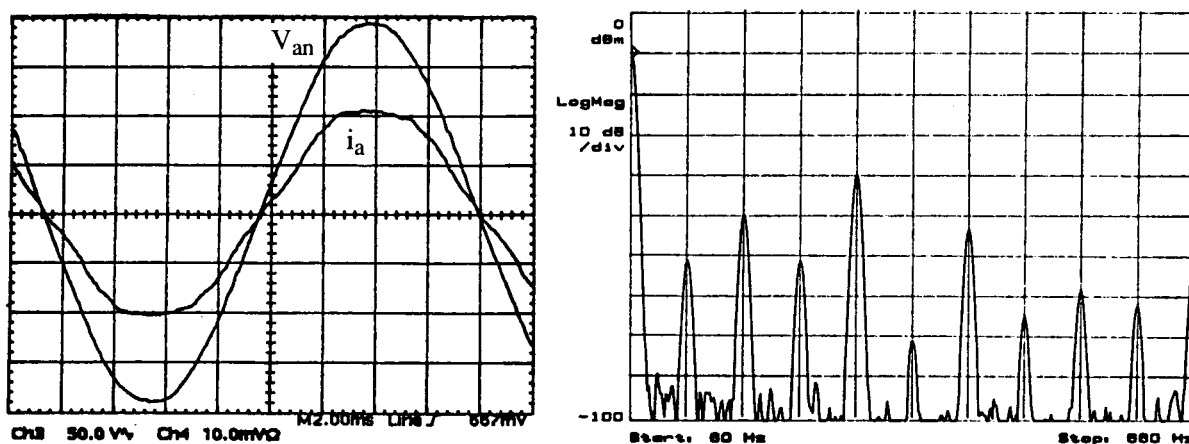


Fig. 7. Measured waveforms (vertical scale: 50 V/div, 5 A/div, and horizontal scale: 2 ms/div) and spectral analysis (vertical scale: 10 dB/div and horizontal scale: 60 Hz/div) of input line current i_a with its ac phase voltage V_{an} for the rectifier at 3-kW output power. The fundamental component of the input current is 7.66 A.

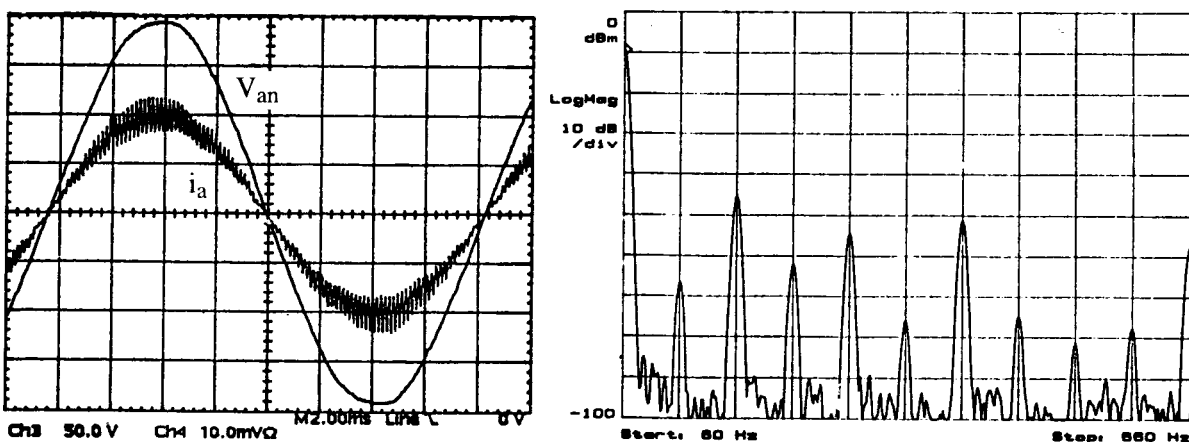


Fig. 8. Measured waveforms (vertical scale: 50 V/div, 1 A/div, and horizontal scale: 2 ms/div) and spectral analysis (vertical scale: 10 dB/div and horizontal scale: 60 Hz/div) of input line current i_a with its ac phase voltage V_{an} for the rectifier at 600-W output power. The fundamental component of the input current is 1.54 A.

The measured rms harmonic currents of the input current are compared with the harmonic limits of the IEEE-519 and IEC555-2 regulations. The results show that the measured harmonic values are quite acceptable for the most applications

and could be further reduced if desired by choosing larger input filter inductances.

Finally, Table III shows the measured efficiency of the rectifier at various operating points. It has the best efficiency of

TABLE I
MEASURED STRESSES OF THE SWITCH AND THE OUTPUT DIODE AT 100%, 50%, AND 10% LOAD

output power [kW]	peak switch voltage [V]	peak input voltage [V]	peak switch current [A]	output current [A]
6	580	340	78	40.8
3	650	340	56	20.5
0.6	670	340	42	4.1
output power [kW]	peak diode voltage [V]	peak input voltage [V]	peak diode current [A]	output current [A]
6	460	340	41	40.8
3	520	340	20.5	20.5
0.6	560	340	4.1	4.1

TABLE II
MEASURED CURRENT HARMONICS AT SEVERAL LOAD CONDITIONS. THE FUNDAMENTAL COMPONENT OF THE INPUT CURRENT IS 14.9 A AT 100% LOAD, 7.66 A AT 50% LOAD, AND 1.54 A AT 10% LOAD

Harmonic number	maximum load (6 kW)	50% load (3 kW)	10% load (600 W)	IEC555-2 Maximum permissible harmonic current	IEEE 519 limits $\frac{I_{\text{short circuit}}}{I_{\text{load}}} < 20$
n	current(rms,A) percent(%)	current(rms,A) percent(%)	current(rms,A) percent(%)		
3	0.09 A/0.6%	0.08 A/1.04%	26 mA/1.67%	2.3 A	4%
5	0.62 A/4.1%	0.24 A/3.13%	9 mA/0.58%	1.14 A	4%
7	0.4 A/2.6%	0.05 A/0.65%	12 mA/0.78%	0.77 A	4%
9	0.03 A/0.20%	0.01 A/0.13%	0.7 mA/0.05%	0.4 A	4%
11	0.08 A/0.54%	0.02 A/0.26%	9 mA/0.58%	0.33 A	4%
2	0.04 A/0.27%	0.02 A/0.26%	2 mA/0.13%	1.08 A	1%
4	0.05 A/0.34%	0.02 A/0.26%	3.5 mA/0.23%	0.43 A	1%
6	0.02 A/0.14%	0.003 A/0.04%	0.5 mA/0.03%	0.3 A	1%
8	0.01 A/0.07%	0.005 A/0.07%	0.5 mA/0.03%	0.23 A	1%
10	0.02 A/0.14%	0.005 A/0.07%	0.5 mA/0.03%	0.184 A	1%
THDs	5.0%	3.4%	2.0%		5%

TABLE III
MEASURED EFFICIENCY OF THE RECTIFIER AT 100%, 50%, AND 10% LOAD

input voltage (L-L, rms) [V]	input current [A]	input power [W]	output voltage [V]	output current [A]	output power [W]	loss [W]	efficiency [%]
239.6	15.6	6486.4	147.1	41.5	6100.5	385.9	94.1
238.9	7.7	3169.6	144.9	20.4	2949.7	219.9	93.1
240.9	1.5	634.2	144.9	3.9	570.7	63.5	90.0

94.1% at the maximum load. Experimental results demonstrate the feasibility of the wide load range with low stresses and high efficiency.

VII. CONCLUSION

In this paper, a new family of three-phase single-switch HPF multiresonant ZCS buck-type rectifiers has been introduced. These rectifiers are capable of drawing a high-quality input-current waveform at nearly unity power factor and have continuous input and output currents. By using a multiresonant scheme, the transistor operates with ZCS, and the diodes

operate with ZVS. Moreover, these rectifiers have a wide load range and low stress on the semiconductor devices.

The input characteristics of these rectifiers are derived and explain well how the open-loop line-current waveform is naturally proportional to the input voltage. The normalized component stresses are derived and presented.

The design and breadboard implementation of a 6-kW single-switch three-phase HPF multiresonant buck rectifier delivering a $147 V_{dc}$ from a 3ϕ 240-V_{rms(L-L)} input has been described. Experimental results demonstrate THD of less than 5% at the full output power, less than 3.5% at the 50% output

power, and less than 2% at the 10% output power in an open-loop rectifier. The rectifier efficiency is about 94% at the full load. The measured rms harmonic currents of the line input current are compared with the harmonic limits of the IEEE-519 and IEC555-2 regulations. The results show that the measured harmonic values are quite acceptable for the most applications and could be further reduced if desired by choosing larger input filter inductances.

REFERENCES

- [1] A. R. Prasad, P. D. Ziogas, and S. Manias, "An active power factor correction technique for three-phase diode rectifiers," in *IEEE Power Electronics Specialists Conf.*, 1989, pp. 58–66.
- [2] E. H. Ismail and R. W. Erickson, "A single transistor three-phase resonant switch for high quality rectification," in *IEEE Power Electronics Specialists Conf.*, 1992, pp. 1341–1351.
- [3] D. S. L. Simonetti, J. Sebastian, and J. Uceda, "Single-switch three-phase power factor preregulator under variable switching frequency and discontinuous input current," in *IEEE Power Electronics Specialists Conf.*, 1993, pp. 657–662.
- [4] J. W. Kolar, H. Ertl, and F. C. Zach, "Space vector-based analytical analysis of the input current distortion of a three-phase discontinuous-mode boost rectifier system," in *IEEE Power Electronics Specialists Conf.*, 1993, pp. 696–703.
- [5] J. Pforr and L. Hobson, "A novel power factor corrected single ended resonant converter with three phase supply," in *IEEE Power Electronics Specialists Conf.*, 1992, pp. 1368–1375.
- [6] E. H. Ismail and R. W. Erickson, "A new class of low cost three-phase high quality rectifiers with zero-voltage switching," in *IEEE Applied Power Electronics Conf.*, 1993, pp. 43–54.
- [7] Y. Jang and R. W. Erickson, "New single-switch three-phase high power factor rectifiers using multi-resonant zero current switching," in *IEEE Applied Power Electronics Conf.*, 1994, pp. 711–717.
- [8] Y. Jang, "Application of resonant technique for three-phase high power factor rectification and integrated magnetic converters," Ph.D. thesis, Univ. Colorado, Boulder, 1995.
- [9] Y. Jang and R. W. Erickson, "Design and experimental results of a 6 kW single-switch three-phase high power factor rectifier using multi-resonant zero current switching," in *IEEE Applied Power Electronics Conf.*, 1996, pp. 524–530.



Yungtaek Jang (S'92–M'95) was born in Seoul, Korea. He received the B.S. degree from Yonsei University, Seoul, Korea, in 1982 and the M.S. and Ph.D. degrees from the University of Colorado, Boulder, in 1991 and 1995, respectively, all in electrical engineering.

From 1982 to 1988, he was a Design Engineer at Hyundai Engineering Corporation, Seoul. From 1995 to 1996, he was a Senior Engineer at Advanced Energy Industries, Inc., Fort Collins, CO. Since 1996, he has been a Senior Design Engineer at Delta Power Electronics Laboratory, Inc., Blacksburg, Virginia. His research interests include resonant power conversion, converter modeling, control techniques, and low harmonic rectification.



Robert W. Erickson (S'80–M'82) was born in Santa Monica, CA, on August 3, 1956. He received the B.S., M.S., and Ph.D. degrees from the California Institute of Technology, Pasadena, in 1978, 1980, and 1983, respectively.

He is presently an Associate Professor in the Department of Electrical and Computer Engineering, University of Colorado, Boulder. His current research directions include converter modeling and control, high-frequency and high-power converter components, and low harmonic rectification.